Journal of Biomechanics 47 (2014) 1689–1695

Contents lists available at ScienceDirect

Journal of Biomechanics

journal homepage: www.elsevier.com/locate/jbiomech
www.JBiomech.com

A periodontal ligament driven remodeling algorithm for orthodontic tooth movement

Junning Chen[a], Wei Li[a], Michael V. Swain[b], M. Ali Darendeliler[b], Qing Li[a,*]

[a] School of Aerospace, Mechanical and Mechatronic Engineering, The University of Sydney, NSW 2006, Australia
[b] Faculty of Dentistry, The University of Sydney, NSW 2006, Australia

ARTICLE INFO

Article history:
Accepted 20 February 2014

Keywords:
Surface remodeling
Orthodontic tooth movement
Periodontal ligament
Hydrostatic stress
Hyperelastic finite element analysis
Maxilla

ABSTRACT

While orthodontic tooth movement (OTM) gains considerable popularity and clinical success, the roles played by relevant tissues involved, particularly periodontal ligament (PDL), remain an open question in biomechanics. This paper develops a soft-tissue induced external (surface) remodeling procedure in a form of power law formulation by correlating time-dependent simulation *in silico* with clinical data *in vivo* ($p < 0.05$), thereby providing a systematic approach for further understanding and prediction of OTM. The biomechanical stimuli, namely hydrostatic stress and displacement vectors experienced in PDL, are proposed to drive tooth movement through an iterative hyperelastic finite element analysis (FEA) procedure. This algorithm was found rather indicative and effective to simulate OTM under different loading conditions, which is of considerable potential to predict therapeutical outcomes and develop a surgical plan for sophisticated orthodontic treatment.

1. Introduction

Orthodontic tooth movement (OTM) is based upon the ability of periodontal ligament (PDL) reaction to appropriate mechanical loading for a remodeling process within dental alveolar bone. OTM relies on a complex set of mechanical stimuli that triggers specific biological reactions in the tissues around the targeted tooth, thereby moving the tooth to a more desired position (Quinn and Yoshikawa, 1985). The 'pressure–tension theory' (Ren et al., 2003; Cattaneo et al., 2005) suggests that tooth movement is a consequence of generating mechanical compression on one side of PDL for bone resorption, and tension on the other side for bone apposition (Ren et al., 2003), in which normal strain in PDL was taken as the mechanical stimulus. Early finite element (FE) studies confirmed the critical role played by PDL (Middleton et al., 1996; Jones et al., 2001), which enabled the estimation of clinical outcomes under a range of orthodontic forces. Nevertheless, the biomechanics behind OTM remains an open question.

Finite element (FE) methods have shown compelling advantages in biomechanical analysis for OTM process (Middleton et al., 1990; Cattaneo et al., 2005; Field et al., 2009), which allows incorporating anatomical, physiological, heterogeneous variance of individuals (Ren et al., 2003). Middleton et al. (1996); Bourauel et al. (1999, 2000), and others (e.g. Qian et al., 2010) pointed out that the mechanical stimuli within PDL were more relevant to OTM than those in the surrounding bones, as the mechanical responses to the orthodontic force in alveolar bone are far below typical thresholds for remodeling to occur. With advances in clinical computerized tomography (CT), sophisticated 3D FE models can be created to precisely quantify biomechanical responses to the initial application of the orthodontic force. However, it remains under-studied as to the understanding of how such responses change during the tooth movement and how to simulate OTM in a time-dependent fashion.

This article aims to address the abovementioned issues through developing an iterative FE procedure driven by a new remodeling rule, in which hydrostatic stress within the PDL and the resultant interfacial displacement are considered as remodeling stimuli to account for the tooth movement. To determine the remodeling parameters, the proposed remodeling simulation is correlated with the clinical data. The remodeling procedure established enables us to gain biomechanical insights into the time-dependent process and explore the effects of different orthodontic loadings *in silico*.

2. Materials and methods

2.1. Clinical data acquisition

14 healthy teenagers (5 boys, 9 girls; mean age, 15.8 years; range from 13.0 to 19.5 years old) who required bilateral extraction of the maxillary first premolars and retraction of the maxillary canines during their orthodontic treatment were

* Correspondence to: Mechanical Engineering Building (J07), Darlington Campus, The University of Sydney, Room S509, NSW 2006, Australia. Tel.: +61 2 9351 8607; fax: +61 2 9351 7060.
E-mail address: qing.li@sydney.edu.au (Q. Li).

http://dx.doi.org/10.1016/j.jbiomech.2014.02.030
0021-9290

recruited. All subjects and their parents or guardians consented to participation after receiving verbal and written explanations (ethics approval: SSWAHS X06-0062 and EK: 358). All the participants had no previous orthodontic or orthopedic treatment histories, no craniofacial anomalies, no previously reported or observed dental treatment on the canine, or any existing medical conditions. After a minimum 3-month consolidation of post-extraction, the distal retraction of maxillary canines was performed with a force of either 0.5 N (namely 50 g in orthodontics, a light force) or 3.0 N (300 g, a heavy force) for each subject, respectively. Measurements were made from the orthodontic impression molds every 28 days from beginning of canine retraction and 4 impressions per patient were obtained at different time points for assessments.

2.2. FE modeling

Oral cone beam CT images (in DICOM format) were captured on one average subject from the group (0.2 mm per pixel resolution) through standard orthodontic measurement. The images were segmented in ScanIP 4.3 (Simpleware Ltd., Exeter UK) (Fig. 1a). Masks of teeth, PDLs, cortical bone, and cancellous bone were created based on their respective Hounsfield unit (HU) (Fig. 1b). Half of the maxilla was set as the region of interest (ROI) for its approximate symmetry in the sagittal plane. These 14 masks (STL format) were further processed in Rhinoceros 4.0 (Robert McNeel & Associates, Seattle USA), to create geometric models with free-form surfaces in non-uniform rational B-splines (NURBs) (Fig. 1c). The solidified models were imported to ABAQUS 6.9.2 (Dassault Systèmes, Tokyo Japan) via IGES files. The unstructured quadratic tetrahedral elements (C3D10H) were used to smoothly capture the anatomical sophistication with an adaptive mesh in a seed size of 2 mm, where mesh-refinement was applied to all 6 PDL regions involved (Fig. 1d). Unlike an initial analysis, the remodeling required updating mesh to follow tooth movement. The average number of elements was 250,000, of which around 40,000 were dedicated to the PDLs. The mesh density was validated through a convergence test as per our previous studies (Li et al., 2004, 2005).

2.3. Material property and loading scenario

The non-linear hyperelastic model was adopted for PDL by fitting the strain–stress curve (Cattaneo et al., 2005), in which the strain energy potential equation (Marlow Model) was interpolated in ABAQUS. The retracted canine was simplified as a rigid body for its negligible deformation compared to PDL. Elastic properties (Table 1) were assigned to the remaining regions in the model (Lettry et al., 2003; Field et al., 2009; Hohmann et al., 2009).

Symmetric boundary conditions were prescribed to the sagittal plane; and full constraints were applied to the coronal and transverse sectional planes (Fig. 2a). The orthodontic force (every 0.5 N from 0.5 N to 3 N, individually) was directly applied through the bracket on the canine surface, pointing towards the second premolar bracket (Fig. 2b). The load direction kept updating step-wise but the magnitude remained constant to simulate an ideal orthodontic spring (Yee et al., 2009). Other factors, such as friction and slipping on the arch wire, or variations in other teeth, have not been considered here for simplification.

2.4. Mechanical stimulus and remodeling algorithm

Physiologically, blood capillaries in the PDL region are exposed to stress and strain induced by orthodontic forces. A certain level of hydrostatic pressure σ_H (Eq. (1)) could collapse capillaries partially or completely, affecting periodontal interstitial fluid (Kristiansen and Heyeraas, 1989) and causing dysfunction of PDL (Hohmann et al., 2009). Therefore, sustained exposure to compression instigates osteoclast recruitment, leading to bone resorption on the compression side (Bourauel et al., 2000). During orthodontic treatment, the volume-averaged hydrostatic pressure $\overline{\sigma}_H$ (Eq. (2)) in PDL indicates the degree of overall disturbance to blood supply (Sarrafpour et al., 2012, Sarrafpour et al., 2013). The previous studies showed that the capillary pressure varies in the root (Field et al., 2010). The upper range of capillary blood pressure, $\sigma_L^*=4.7$ kPa (35 mmHg) (Kristiansen and Heyeraas, 1989, Hohmann et al., 2007), was adopted here as a threshold to trigger the remodeling activities (Hohmann et al., 2009).

$$\sigma_H=\frac{1}{3}(\sigma_{xx}+\sigma_{yy}+\sigma_{zz}) \tag{1}$$

$$\overline{\sigma}_H=\frac{\sum_e \sigma_H^e V^e}{\sum_e V^e} \tag{2}$$

Furthermore, the localized PDL displacement at the interface between the tooth and PDL was considered to direct tooth movement (Bourauel et al., 1999, 2000; Qian et al., 2010), in which the unit vector $\mathbf{n}$ was computed as Eq. (3). In this equation, $\mathbf{u}$ was the nodal displacement and $\mathbf{u}^{max}$ indicated the maximum. The unit vectors on the surface nodes preserved a constant tooth profile.

$$\mathbf{n}=\frac{\mathbf{u}}{|\mathbf{u}^{max}|} \tag{3}$$

Table 1
Material properties adopted in tooth movement simulation.

Material	Young's Modulus (MPa)	Poisson's Ratio
Other teeth	20,000	0.20
Cortical bone	15,750	0.33
Cancellous bone	1,970	0.33
PDL	Hyperelastic (Marlow)	0.45

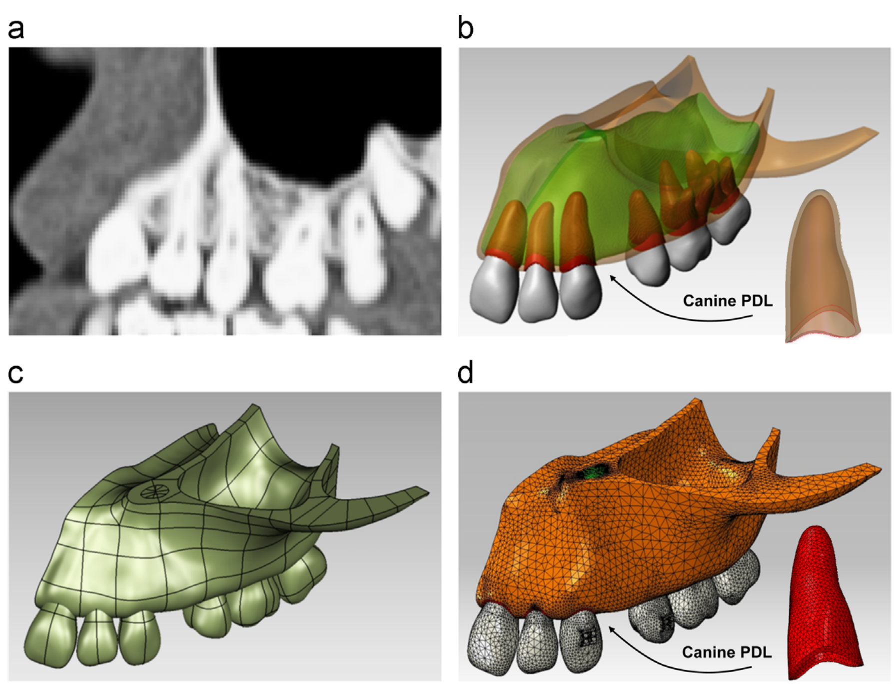

Fig. 1. (a) CT images captured in DICOM format; (b) masks created for each individual component in ScanIP; (c) NURBS surfaces created in Rhinoceros to form solidified geometric models; and (d) meshed FE models in ABAQUS for analysis.